Development of a New Laboratory Test Methodology for Rapid Ageing of HVAC Filters

Chunxu HUANG[1], Ta-Kuan CHUANG[1], Iane GOMES[2], Laura AJALA[3], Elliot P. CRAM[1], Nusrat JUNG[1], Brandon E. BOOR[1]*

[1]Purdue University, Lyles School of Civil Engineering, West Lafayette, Indiana, United States
[2]Universidade Federal do Rio de Janeiro, Brazil
[3]Universidade Estadual de Campinas, Brazil

* Corresponding Author (email: bboor@purdue.edu)

ABSTRACT

Air filters installed in residential and commercial HVAC systems encounter a complex mixture of aerosols of outdoor and indoor origin during their service life. Standardized laboratory test methodologies are important for evaluating the loading behavior of HVAC filters. Loading aerosols commonly used to age HVAC filters include various test dusts (ISO-12103-1-A2, ISO-12103-1-A4, ASHRAE Test Dust) that are primarily composed of coarse mode particles (1 to 100 µm). However, urban aerosol mass size distributions often feature a prominent accumulation mode between 0.1 and 1 µm that is not well represented by traditional loading aerosols. The aim of this study is to develop a new laboratory test methodology for rapid ageing of HVAC filters with a representative urban aerosol mass size distribution at a high concentration to better predict long-term changes in HVAC filter performance. A HVAC filter test rig was custom designed and built following ASHRAE 52.2 specifications to artificially age HVAC filters with sub-micron potassium chloride (KCl) aerosol produced by a thermal aerosol generator. The KCl aerosol is formed by burning KCl sticks in a high temperature oxygen-propane flame and is delivered to the test rig via a damper-controlled intake duct. The results demonstrate that the new sub-micron KCl loading aerosol is a time- and cost-effective technique to artificially age HVAC filters with a particle mass size distribution representative of that found in HVAC installations in buildings.

1. INTRODUCTION

Indoor air quality plays a critical role in affecting human health and well-being as people spend the majority of their time indoors. Exposure to airborne particles of outdoor and indoor origin can cause adverse human health outcomes, such as respiratory, cardiovascular, and allergic diseases. Outdoor particles can enter buildings through mechanical and natural ventilation and infiltration across the building envelope. Under mechanical ventilation, outdoor particles are introduced to the indoor environment via HVAC systems. Outdoor particle size distributions (PSDs) in urban areas are often dominated by sub-micron particles on both a mass- and number-basis (Wu & Boor, 2021). Outdoor mass PSDs typically feature a prominent accumulation mode between 100 and 1,000 nm. Similarly, indoor PSDs are often dominated by sub-micron particles on both a mass- and number-basis, due to indoor particle production via cooking, combustion, and secondary organic aerosol formation due to terpene ozonolysis (Jiang et al., 2021a; Jiang et al., 2021b; Patra et al., 2024).

Air filtration in HVAC systems is widely employed to reduce concentrations of particles of outdoor and indoor origin in buildings (Azimi et al., 2016; Ben-David et al., 2018; English 2016; He et al., 2014; Riley et al., 2002). While HVAC filters can improve indoor air quality, they can contribute to the energy usage of HVAC systems. Initially, clean (unaged) filters operate efficiently due to their low airflow resistance (filter pressure drop, ΔP), thereby contributing little to blower/fan energy consumption. As HVAC filters age, the accumulation of particles within the filter media restricts airflow, leading to a rise in the filter ΔP. This increase in filter ΔP can result in reduced ventilation airflow rates for fixed-speed blowers. Variable-speed blowers may experience higher energy consumption in order to overcome the elevated filter ΔP and sustain consistent ventilation airflow rates in HVAC systems (Li & Siegel, 2020; Stephens et al., 2010).

In-situ studies have been conducted to evaluate long-term changes in HVAC filter performance and associated blower/fan energy use (Alavy et al., 2020; Alavy & Siegel, 2020; Ben-David et al., 2018; Li & Siegel, 2019; Owen et al., 2014; Walker et al., 2013; Zaatari et al., 2014; Zhang et al., 2020). In-situ testing offers a basis for a realistic assessment of HVAC filter loading behavior; however, it is time- and cost-intensive due to the long duration of the measurements (e.g.

1 to 2 years). In contrast, laboratory-based testing provides a standardized approach to evaluate HVAC filter loading, allowing for accelerated and reproducible assessments of long-term filter performance. Therefore, laboratory-based testing methods are essential for rigorously evaluating HVAC filter performance across various filter designs.

Commonly used loading aerosols in laboratory-based HVAC filter test procedures include various test dusts (ISO-12103-1-A2, ISO-12103-1-A4, ASHRAE Test Dust) that are primarily composed of coarse mode particles (1 to 100 µm). Such test dusts are not an accurate reflection of the mass and number PSDs commonly reported for outdoor (urban) and indoor air (Corbat et al., 2007; Tronville, 2005). New laboratory-based filter test procedures should include a loading aerosol that better simulates that found in outdoor and indoor atmospheric environments. Specifically, a sub-micron loading aerosol is needed that better reproduces the prominent accumulation mode (100 to 1,000 nm) found in mass PSDs in outdoor urban environments. Compared with super-micron test dusts, smaller sub-micron particles can pass through the pores of the filter media, leading to particle accumulation within the depth of the filter material instead of just at the front-facing surface of the filter (Abdolghader et al., 2018; Wang & Otani, 2013). Depth filtration induced by sub-micron particles can lead to an accelerated increase in the filter ΔP compared to surface filtration.

The study develops a new laboratory-based methodology for rapid ageing of HVAC filters with a representative urban aerosol mass PSD at high concentration. The chosen loading aerosol generation technique, a thermal aerosol generator (TAG), utilizes evaporation-condensation of salt vapor to produce sub-micron salt particles at a high mass production rate and reasonable cost (Wu & Boor, 2020). This enables rapid ageing of HVAC filters with a mass PSD similar to that found in outdoor urban environments. By exposing HVAC filters to very high mass concentrations of sub-micron particles, the proposed testing method can simulate the long-term effects of in-situ filter loading in a short period of time. A newly designed TAG (Series 6000, SFP Services Ltd., UK) that can produce mass PSDs with a modal diameter of around 150 nm was selected for this study. The aerosol output of the TAG was systematically evaluated by Wu & Boor (2020). A HVAC filter test rig was custom designed and built following ASHRAE Standard 52.2 specifications to artificially age HVAC filters with sub-micron salt aerosol produced by the TAG. The outcome of this study will inform the development of ASHRAE Guideline 35: Method for Determining the Energy Consumption Caused by Air-Cleaning and Filtration Devices. To evaluate the new laboratory-based methodology for rapid ageing of HVAC filters, three different Minimum Efficiency Reporting Value (MERV)-rated filters (MERV8, MERV13, and MERV14) were evaluated. The reproducibility and repeatability of the new methodology was evaluated under different loading conditions, including the aerosol mass production rate of the TAG, volumetric airflow rates, and relative humidity (RH).

2. MATERIALS AND METHODS

2.1 Thermal Aerosol Generator

A schematic of the TAG is shown in Figure 1**Error! Reference source not found.**. High mass concentrations of sub-micron potassium chloride (KCl) particles are generated by vaporizing KCl sticks within an oxy-propane flame. An in-depth characterization of this aerosol generation technique was performed by Wu & Boor (2020). Overall, the number and mass PSD output of the TAG closely resembles those found in outdoor urban environments, but at significantly higher concentrations. The output aerosol number and mass PSDs can be regulated to some extent by adjusting the operational settings of the TAG, such as the salt stick feed rate, salt stick content (KCl or sodium chloride (NaCl)), and salt stick diameter. Among these settings, the salt stick feed rate has the most significant impact on the shape of the PSDs. As the feed rate increases, the prominent peaks of the number and mass PSDs shift towards larger particle sizes for KCl and NaCl sticks (Wu & Boor, 2020).

2.2 Purdue University HVAC Filter Test Rig

The rapid HVAC filter ageing experiments with the TAG were conducted in a full-scale HVAC filter test rig, as shown in Figure 1 and Figure 2. The length of the HVAC filter test rig is 28 ft, with a square cross section of 2×2 ft. A high-capacity tubular inline centrifugal blower (Model TSL122, Twin City Fans & Blowers Ltd., Plymouth, MN, USA) was installed at the end of the test rig to draw in air. A variable frequency driver (VFD) (Series SMV, Lenze SE, Glendale Heights, IL, USA) controlled the blower motor's rotation speed and volumetric airflow rate. The VFD voltage control feature allowed for feedback control of the motor speed based on air resistance and volumetric airflow rate setpoints. The test rig was also equipped with a large-scale steam humidifier (Model EC-10, PURE Humidifier Co., Chaska, MN, USA) with a maximum moisture output of 30 lb h^{-1}, compatible with a voltage control for feedback.

A MERV8 filter was installed at the intake of the test rig to protect the downstream apparatus from coarse particles in the laboratory air. The ejection tube for the moisture output from the steam humidifier was installed after the MERV8 intake

filter. The sub-micron KCl particles generated by the TAG were drawn into the ventilation duct through a 90° elbow on the top side of the duct. The elbow was covered in insulation for safety and the intake volume was regulated by a damper. A test filter bank was custom-designed to fit different configurations of test filters. Aerosol sampling probes were installed upstream and downstream of the test filter bank. The aerosol sampling system was controlled by a solenoid valve to alternate the sampling location between upstream and downstream at a fixed time interval. The in-duct volumetric airflow rate was measured using a self-averaging pitot tube array of five pitot tubes (Model 160-8, Dwyer Instruments Inc., Michigan City, IN, USA) in a diagonal line across the ventilation duct, as recommended in ASHRAE Standard 41.2 (Hall et al., 2018). To avoid clogging of the pitot tubes, a self-cleaning system was employed to periodically clean the pitot tubes with particle-free compressed air. An exhaust fume hood was placed at the end of the HVAC filter test rig to expel any remaining sub-micron KCl aerosol outdoors to prevent the loading aerosol from entering the laboratory air.

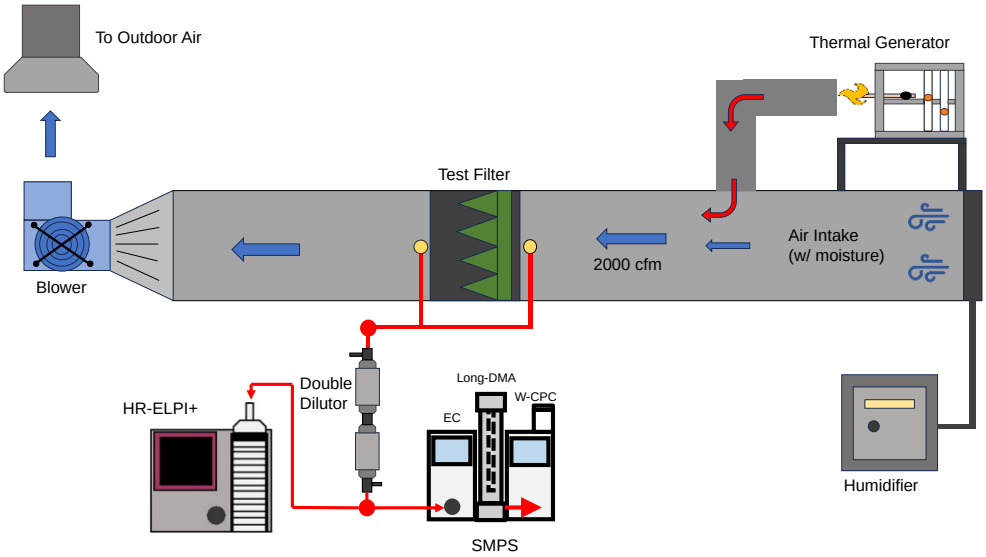

Figure 1: Schematic of the Purdue University HVAC filter test rig.

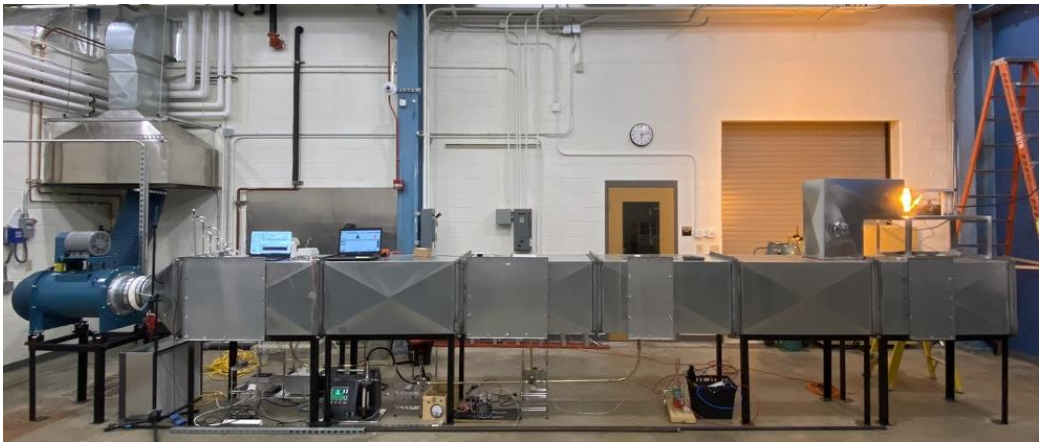

Figure 2: Photo of the Purdue University HVAC filter test rig.

2.3 HVAC Filter Loading Experimental Protocol

Detailed characterization of the stability and reproducibility of the sub-micron KCl aerosol output of the TAG and operational conditions of the HVAC filter test rig (volumetric airflow rate, RH, and in-duct airflow uniformity) are needed to ensure the robustness of the new laboratory-based methodology for rapid ageing of HVAC filters. To measure the KCl aerosol across the test filter, a scanning mobility particle sizer (SMPS) (Model 3938NL88, TSI Inc., Shoreview, MN, USA) and a high-resolution electrical low-pressure impactor (HR-ELPI+) (Model 2E10-10, Dekati Ltd., Kangasala, Finland) with sintered collection plates were used. The SMPS measured the electrical mobility diameter (D_{em})-based number PSDs and the HR-ELPI+ measured the aerodynamic diameter (D_a)-based number PSDs of the KCl aerosol. The SMPS includes an electrostatic classifier (Model 3082, TSI Inc., Shoreview, MN, USA), consisting of a Kr-85 bi-polar charger (370 MBq, Model 3077A, TSI Inc., Shoreview, MN, USA) and a long differential mobility analyzer (DMA)

(Model 3081, TSI Inc., Shoreview, MN, USA), and a water-based condensation particle counter (CPC) (Model 3788, TSI Inc., Shoreview, MN, USA). The SMPS first charges particles using the bi-polar charger into a known charge distribution. The charged particles are then classified by an electric field within the long DMA. The electrical mobility-classified particles are then counted by the CPC via optical detection. The scan time of the SMPS was set to be 4 minutes during the loading experiments for particles from D_{em} = 17 to 1,000 nm. The HR-ELPI+ first charges particles using a uni-polar charger and then classifies particles through inertial impaction as particles pass through a cascade impactor. Charged particles are detected following impaction onto sintered collection plates via sensitive electrometers. The HR-ELPI+ sampled particles at 1 Hz from D_a = 6 to 10,000 nm. An aerosol dilution system was developed to reduce the aerosol concentration prior to measurement with the SMPS and HR-ELPI+. A double-dilutor system was built by two connecting ejector dilutors in series (Dekati Dilutor, Dekati Ltd., Kangasala, Finland). The nominal dilution factor was 8.18 for each individual dilutor. Experimental verification was conducted to confirm the actual dilution factor during the experiments.

The ΔP across the test filter was measured via custom-built static pressure taps connected to digital pressure transducers (Series 265, Setra Systems Inc., Boxborough, MA, USA) that are integrated with data acquisition hardware (Model 6211, National Instruments Inc., Austin, TX, USA) and LabVIEW software (Version 2020, National Instruments Inc., Austin, TX, USA). The data acquisition system was also used for automation of various key parameters of the test rig through application of proportional-integral-derivative (PID) control algorithms. These parameters included the blower motor's rotation speed, steam humidifier moisture output, and switching of the aerosol sampling valve, among others.

Four sensitivity test categories were considered for evaluation of the new laboratory-based methodology for rapid ageing of HVAC filters: (1.) baseline tests, (2.) volumetric airflow rate sensitivity tests, (3.) salt stick feed rate sensitivity tests, and (4.) RH sensitivity tests. Repeated tests were done under the same experimental conditions to validate the repeatability of the loading methodology. For the baseline tests, five tests were completed under the same conditions for each MERV category (MERV8, MERV13, MERV14). Triplicate tests were done for each sensitivity test category. The experimental conditions for the baseline test were as follows: (1.) volumetric airflow rate of 2000 $ft^3\ min^{-1}$ (3398 $m^3\ h^{-1}$), (2.) RH of 42.5 ± 2.5%, and (3.) salt stick feed rate on the TAG of 10 mm min^{-1}. There were two more volumetric airflow rate settings for the airflow sensitivity tests: 500 $ft^3\ min^{-1}$ and 1000 $ft^3\ min^{-1}$. Similarly, for the salt stick feed rate sensitivity tests, 5 mm min^{-1} and 18 mm min^{-1} were evaluated and for the RH sensitivity tests, 27.5 ± 2.5% and 57.5 ± 2.5% were evaluated.

3. RESULTS AND DISCUSSION

3.1 Characterization of the Thermal Aerosol Generator

A number PSD time-series from a MERV14 baseline loading experiment is shown in Figure 3 as an illustrative example. Sub-micron KCl aerosol produced by the TAG were measured with the HR-ELPI+ upstream and downstream of the MERV14 filter at 3 min intervals. The difference in the upstream and downstream KCl aerosol number concentrations is evident due to particle removal by the MERV14 filter. Overall, the sub-micron KCl loading aerosol output from the TAG was consistent and stable throughout the loading experiments in the HVAC filter test rig. Periodic fluctuations were observed due to variations in the operational state of the TAG or airflow conditions within the test rig.

A statistical analysis of the number, surface area, volume, and mass PSDs of the artificially-generated KCl particles across all baseline experiments is shown in Figure 4. The curve in black color is the median PSD and the shaded area under and above the curve represents the 25th to 75th percentile range. A bi-modal lognormal distribution function fitting ($\frac{dN}{dLogD_p}$, cm^{-3}) (Wu & Boor, 2021) was performed for the median PSD. The geometric mean diameter ($\overline{D_{p,i}}$), geometric standard deviation (σ_i), and particle number concentration or amplitude (N_i) for each mode (i) were determined and the results are shown side-by-side with measured PSDs.

$$\frac{dN}{dLogD_p} = \sum_{i=1}^{2} \frac{N_i}{(2\pi)^{\frac{1}{2}} \log(\sigma_i)} \exp\left[-\frac{\left(log\ D_p - log\ \overline{D_{p,i}}\right)^2}{2log^2(\sigma_i)}\right] \quad (1)$$

The number PSDs obtained from the bi-modal lognormal distribution function fitting were translated into surface area PSDs ($\frac{dS}{dLogD_p}$, $\mu m^2\ cm^{-3}$), volume PSDs ($\frac{dV}{dLogD_p}$, $\mu m^3\ cm^{-3}$) assuming spherical particles, and mass PSDs ($\frac{dM}{dLogD_p}$, $\mu g\ m^{-3}$) using a constant bulk KCl particle density of ρ_p = 1.98 g cm^{-3} (Wu & Boor, 2020). Bi-modal lognormal distribution function fitting parameters are summarized in 1. The width of the prominent mode in the measured number PSDs is small, typically with a σ_i = 1.2 to 1.5 for each mode.

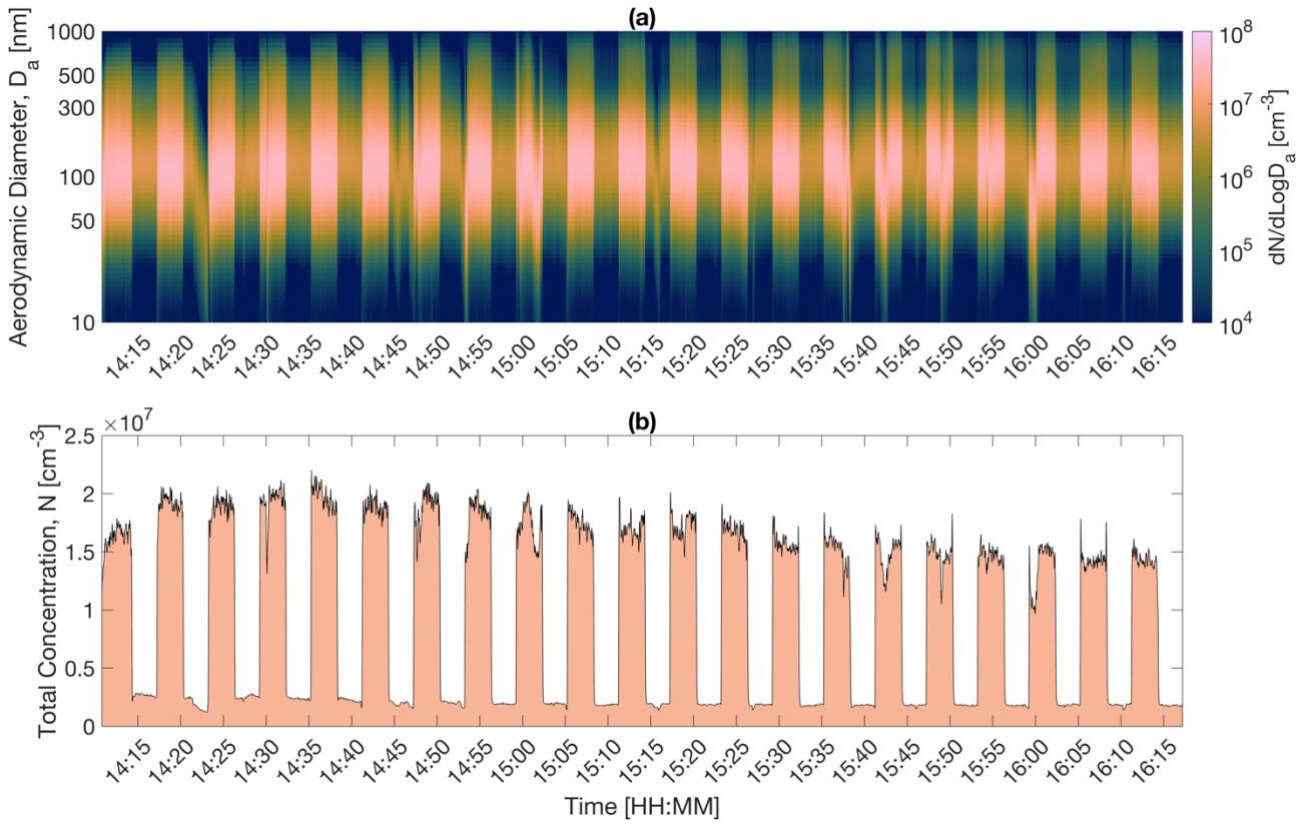

Figure 3: Sub-micron KCl (a.) aerosol number PSD and (b.) size-integrated number concentration time-series as measured by the HR-ELPI+ during a MERV14 baseline loading experiment in the HVAC filter test rig.

Table 1: Bi-modal lognormal distribution function fitting parameters for each PSD type.

PSD Type	Mode 1			Mode 2		
	Modal Amplitude N_1, S_1, V_1, M_1	**Modal Diameter $\overline{D_{p,1}}$ [nm]**	**Geometric Standard Deviation σ_1 [-]**	**Modal Amplitude N_2, S_2, V_2, M_2**	**Modal Diameter $\overline{D_{p,2}}$ [nm]**	**Geometric Standard Deviation σ_2 [-]**
Number	1.0×10^7 cm^{-3}	84.4	1.49	1.5×10^6 cm^{-3}	130.4	1.28
Surface Area	2.43×10^5 μm^2 cm^{-3}	107.2	1.43	1.35×10^5 μm^2 cm^{-3}	151.7	1.27
Volume	4.41×10^4 μm^3 cm^{-3}	119.5	1.42	3.69×10^3 μm^3 cm^{-3}	161.7	1.27
Mass	8.73×10^3 μg m^{-3}	119.5	1.42	7.31×10^3 μg m^{-3}	161.7	1.27

3.2 Characterization of Volumetric Airflow Rates in the HVAC Filter Test Rig

Stable volumetric airflow rates were achieved across all airflow settings (500 ft^3 min^{-1}, 1000 ft^3 min^{-1}, 2000 ft^3 min^{-1}) in the HVAC filter test rig via implementation of the self-averaging pitot tube array and the PID controller system for the blower VFD. **Figure 5** illustrates three real-time in-duct volumetric airflow rate measurements at different setpoints. Small fluctuations can be seen for all setpoints; this can be due to noise in the sensor signals and the intrinsic drawbacks associated with the PID controller. The narrow 25th to 75th percentile range indicates the overall stability of the in-duct volumetric airflow rates and the repeatability of the experimental results. For all airflow setpoints, the median volumetric airflow rates complied with the ASHRAE Standard 52.2 requirement of maintaining the airflow at ±2% of the setpoint (Corbat et al., 2007). The increased variation for the 500 ft^3 min^{-1} and 1000 ft^3 min^{-1} setpoints are due to the increased measurement uncertainty of the pitot tubes under low air velocity conditions (Folsom 1956; Klopfenstein 1998).

3.3 Characterization of RH in the HVAC Filter Test Rig

Similarly, illustrations of in-duct RH measurements are shown in Figure 6. The in-duct temperature was raised due to the flame-induced heat once the TAG starts. Consequently, elevated RH can be observed at the beginning of the experiments,

which gradually decreased due to the increasing in-duct temperature. The periodic dips in the RH measurement were due to the humidifier tank automatically refilling with the cold water supply, which briefly suppressed the boiling process.

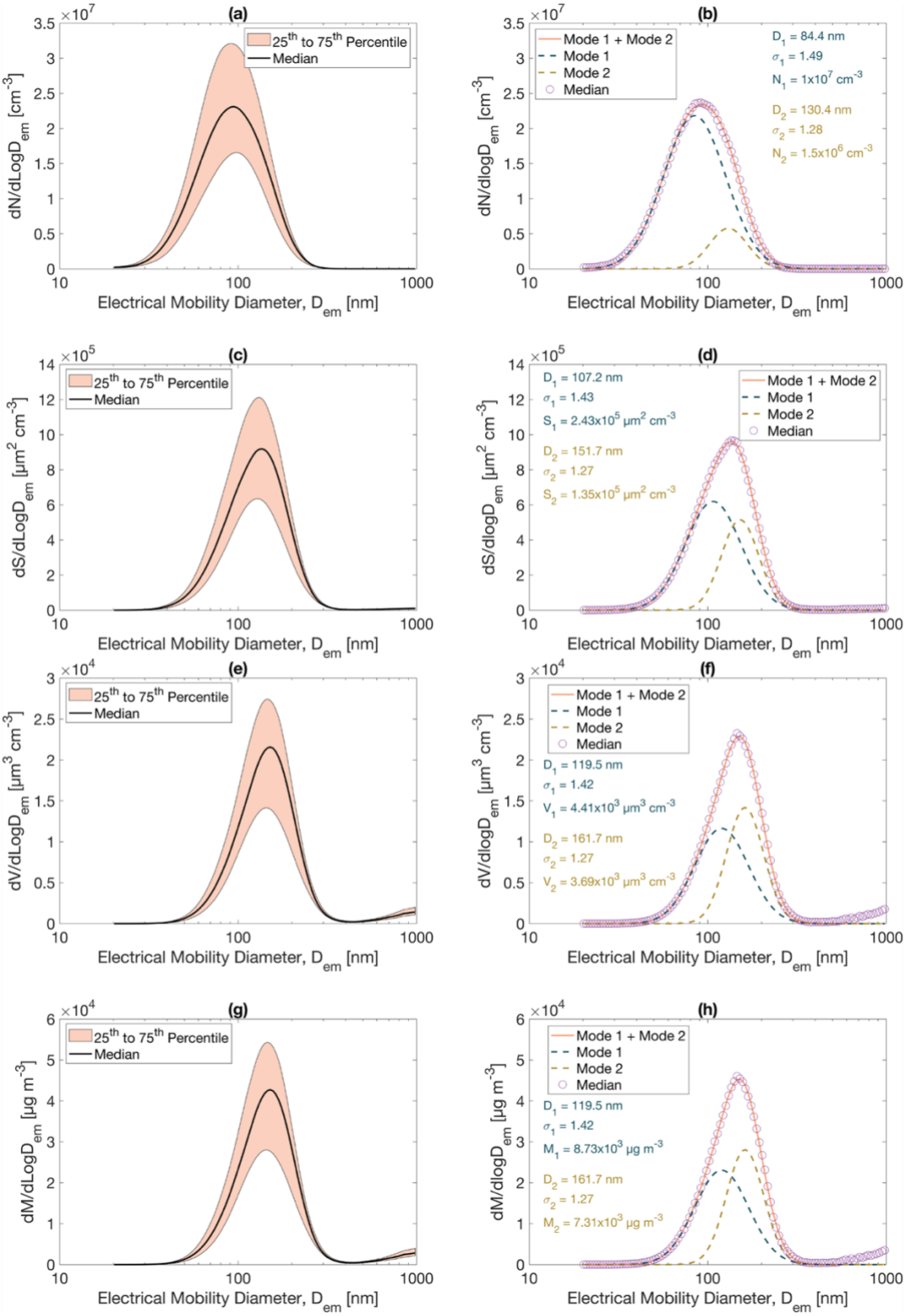

Figure 4: Number (a. and b.), surface area (c. and d.), volume (e. and f.), and mass (g. and h.) PSDs for the sub-micron KCl aerosol as measured in the HVAC filter test rig. The black curve represents the median PSD, and the shaded area represents the 25th to 75th percentile range. Bi-modal lognormal distribution function fitting parameters are listed.

The median RH values are very close to the desired RH setpoints. The narrow 25th to 75th percentile range indicates an acceptable level of stability for in-duct RH control. A tighter RH range (±2.5% RH) was needed for the new loading methodology compared to that specified in ASHRAE Standard 52.2 (±10% RH) (Corbat et al., 2007) as variations in the median RH greater than ±2.5% of the setpoint resulted in inconsistent loading periods as observed in preliminary tests.

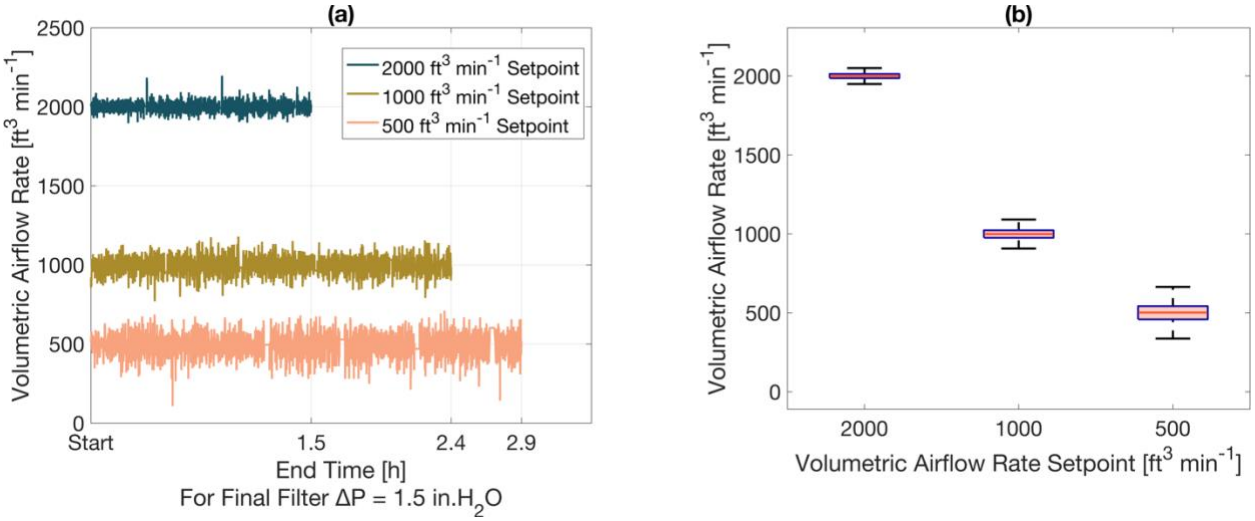

Figure 5: Evaluation of in-duct volumetric airflow rates at different setpoints: (a.) time-series measurement and (b.) box plots showing the median and 25th and 75th percentile range. The variation in the HVAC filter loading end times is attributed to the different volumetric airflow rate setpoints. The measurements are for a MERV14 filter with a 10 mm min^{-1} salt stick feed rate and 42.5 ± 2.5% RH.

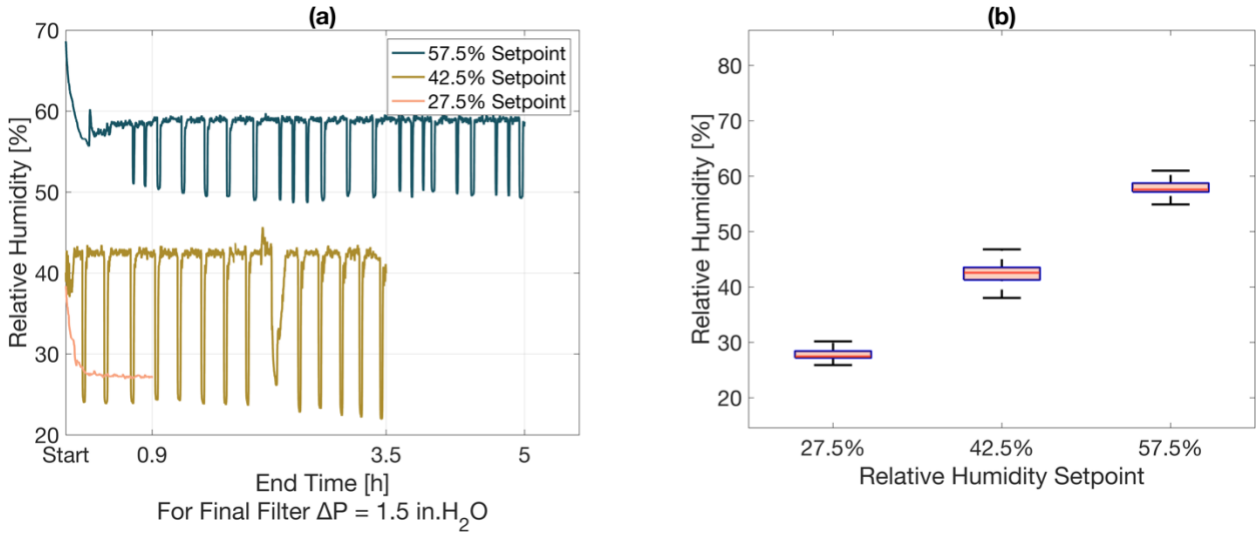

Figure 6: Evaluation of in-duct RH at different setpoints: (a.) time-series measurement and (b.) box plots showing the median and 25th and 75th percentile range. The variation in the HVAC filter loading end times is attributed to the different RH setpoints. The measurements are for a MERV14 filter with a 10 mm min^{-1} salt stick feed rate and 2000 ft^3 min^{-1} volumetric airflow rate.

3.4 Characterization of Airflow and KCl Aerosol Uniformity in the HVAC Filter Test Rig

Uniformity measurements of the airflow velocity and sub-micron KCl aerosol concentrations were performed on a nine-point traverse across the ventilation ductwork (Corbat et al., 2007). Figure 7 illustrates the total size-integrated number concentrations of KCl aerosol and airflow velocities at each of the nine traverse points. Higher particle number concentrations and airflow velocities can be seen towards points 3, 6, and 9, indicating that this side of the test filter will be exposed to a greater quantity of loading aerosol. Overall, sufficient uniformity was achieved for airflow velocities with

a COV = 5.2%, which meets the AHSRAE Standard 52.2 specifications of COV < 10% for airflow velocity. A COV of 20.7% for the KCl aerosol number concentration uniformity was obtained, which is slightly higher than the AHSRAE Standard 52.2 specification of COV < 15% for loading aerosol concentrations (Corbat et al., 2007).

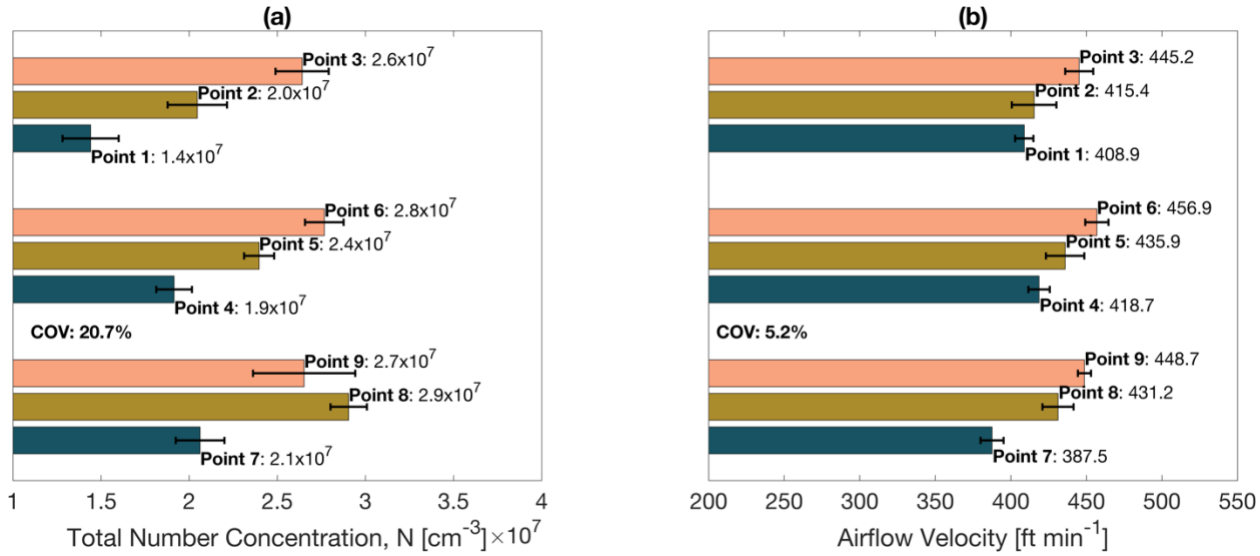

Figure 7: Uniformity measurements for: (a.) KCl aerosol number concentrations and (b.) airflow velocities.

3.5 Evaluation of KCl Aerosol Deposition and Dilution in the Aerosol Sampling Manifold

The KCl aerosol sampling manifold includes the sample plumbing needed to carry the aerosol sample from the HVAC filter test rig to the SMPS and HR-ELPI+ for PSD measurement. During aerosol transport in the sampling manifold, particles can be removed due to various deposition mechanisms, including: (1.) inlet efficiency, η_{inlet}: particle loss at the sample probe inlet caused by different airflow velocities between the sample line airflow and in-duct airflow; (2.) efficiency for gravitational settling in the sample line, $\eta_{tube,grav}$: particles deposit on sample line walls due to gravitational forces; (3.) efficiency for diffusional deposition in the sample line, $\eta_{tube,diff}$: particles diffuse from the high concentration sample airflow stream to low concentrations along with sample line walls due to Brownian motion; and (4.) inertial deposition at a bend in the sample line, $\eta_{inert,bend}$: particles deviate from the airflow stream and deposit on the sample line walls during airflow redirection through a bend. The total aerosol sample transport efficiency is defined as the product of each mechanism. Figure 8 illustrates the size-resolved total aerosol sample transport efficiencies ranging from D_a = 6 to 1,000 nm. The sampling system established transport efficiencies above 0.9 across the entire particle size range of interest for the sub-micron KCl aerosol, meaning that there is minimum particle loss in the sampling system. The transport efficiencies for larger particles (> 100 nm) are slightly above 1 for 1000 and 2000 ft^3 min^{-1}, which is due to the sub-isokinetic sampling effects caused by the in-duct airflow velocity being higher than the sample line airflow velocity.

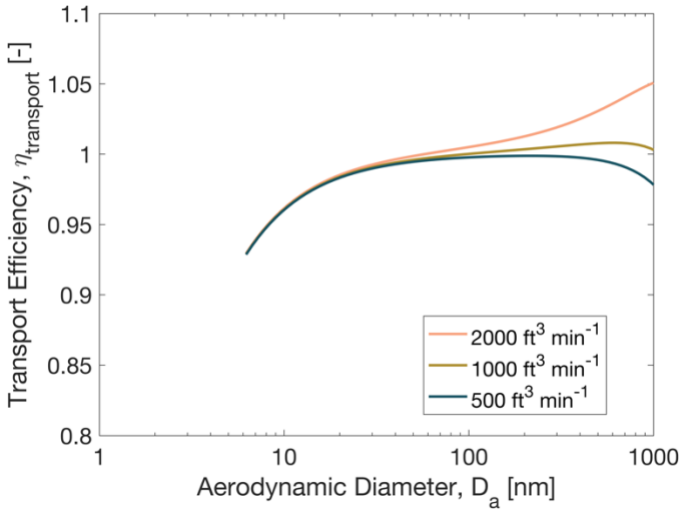

Figure 8: Total sample aerosol transport efficiencies in the sampling manifold of the HVAC filter test rig.

In addition to deposition losses in the sampling manifold, the dilution factor of the double-dilutor system used upstream of the SMPS and HR-ELPI+ was experimentally determined by employing a CPC that measured particle number concentrations before and after dilution. The measured dilution factor was found to be 65.6, which agreed closely with the nominal value of 66.9 for the two ejector dilutors in series. This dilution amount was sufficient to bring the sample aerosol number concentrations to within an acceptable range for measurement by the SMPS and HR-ELPI+.

4. CONCLUSIONS

A new laboratory-based methodology for rapid ageing of HVAC filters with a representative urban aerosol mass PSD at high concentration was developed and characterized in this study. The method utilizes a TAG to produce high concentrations of sub-micron KCl aerosol with mass PSDs that closely resemble those observed in outdoor urban environments. Stability in the KCl aerosol output of the TAG was observed from the measured PSD time-series. The number, surface area, volume, and mass PSDs of the KCl loading aerosol were evaluated and demonstrated that the TAG can provide a repeatable aerosol output with a narrow and tightly controlled PSD. The TAG provides a basis to better simulate in-situ loading conditions for HVAC filters exposed to sub-micron particles. The high mass concentration allows for time-efficient loading tests of HVAC filters in the laboratory. Furthermore, the physical parameters of the HVAC filter test rig were evaluated, including the volumetric airflow rate, RH, and the airflow and aerosol uniformity. In general, stable airflow conditions in the test rig were achieved. A tighter RH control beyond that specified in ASHRAE Standard 52.2 was needed to ensure repeatability of HVAC filter loading results; this tight control was successfully obtained through use of a steam humidifier and PID control. The uniformity measurements resulted in low COV values for airflow velocities and KCl number concentrations, indicating unbiased loading results for HVAC filters. KCl aerosol transport loss through the sampling manifold was minimal; this ensured reliable aerosol measurement with the SMPS and HR-ELPI+. The dilution factor of the double-dilutor system was experimentally determined and found to be adequate for diluting the high concentration of artificially-generated KCl loading aerosol to a satisfactory level to avoid overloading the aerosol instrumentation. The new laboratory-based methodology for rapid ageing of HVAC filters is a time- and cost-effective solution for ASHRAE Guideline 35 for evaluating the blower/fan energy implications of aged HVAC filters.

REFERENCES

Abdolghader, P., et al (2018). Airborne nanoparticles filtration performance of fibrous media: A review. *Science and Technology for the Built Environment*, *24*(6), 648–672.

Alavy, M., et al (2020). Energy use in residential buildings: Analyses of high-efficiency filters and HVAC fans. *Energy and Buildings*, *209*.

Alavy, M., et al (2020). In-situ effectiveness of residential HVAC filters. *Indoor Air*, *30*(1), 156–166.

Azimi, P., et al (2016). Modeling the impact of residential HVAC filtration on indoor particles of outdoor origin (RP-1691). *Science and Technology for the Built Environment*, *22*(4), 431–462.

Ben-David, T., et al (2018). Measuring the efficacy of HVAC particle filtration over a range of ventilation rates in an office building. *Building and Environment*, *144*(August), 648–656.

Corbat, M. D., et al (2007). Method of testing general ventilation air-cleaning devices for removal efficiency by particle size. *ASHRAE Standard*, *2017*(STANDARD 52.2), 1–64.

English, T. R. (2016). Selecting ventilation air filters to reduce PM2.5 of outdoor origin. *ASHRAE Journal*, *58*(11), 8–10.

Folsom, R. G. (1956). Review of the Pitot Tube. *Journal of Fluids Engineering*, *78*(7), 1447–1460.

Hall, R. L., et al (2018). Standard Methods for Air Velocity and Airflow Measurement. *Ashrae Standard*, *2018*(Standard 41.2).

He, C., et al (2014). Evaluation of filter media performance: Correlation between high and low challenge concentration tests for toluene and formaldehyde (ASHRAE RP-1557). *HVAC and R Research*, *20*(5), 508–521.

Jiang, J., et al (2021a). Real-Time Measurements of Botanical Disinfectant Emissions, Transformations, and Multiphase Inhalation Exposures in Buildings. *Environmental Science and Technology Letters*, *8*(7), 558–566.

Jiang, J., et al (2021b). Using Building Energy and Smart Thermostat Data to Evaluate Indoor Ultrafine Particle Source and Loss Processes in a Net-Zero Energy House. *ACS ES&T Engineering*, *1*(4), 780–793. h

Klopfenstein, R. (1998). Air velocity and flow measurement using a Pitot tube. In *ISA Transactions* (Vol. 37, Issue 4, pp. 257–263).

Li, T., et al (2020). Laboratory performance of new and used residential HVAC filters: Comparison to field results (RP-1649). *Science and Technology for the Built Environment*, *26*(6), 844–855.

Li, T., et al (2019). In situ efficiency of filters in residential central HVAC systems. *Indoor Air*, *November 2019*, 315–325.

Owen, K., et al (2014). How do pressure drop, efficiency, weight gain, and loaded dust composition change throughout filter lifetime? In *ASHRAE Transactions* (Vol. 120, Issue PART 1, pp. 366–381).

Patra, S. S., et al (2024). Dynamics of nanocluster aerosol in the indoor atmosphere during gas cooking. *PNAS Nexus*, *3*(2), 1–11.

Riley, W. J., et al (2002). Indoor particulate matter of outdoor origin: Importance of size-dependent removal mechanisms. *Environmental Science and Technology*, *36*(2), 200–207.

Stephens, B., et al (2010). The effects of filtration on pressure drop and energy consumption in residential hvac systems (rp-1299). *HVAC and R Research*, *16*(3), 273–294.

Tronville, P. (2005). *Filters for Vehicular*. *September*, 24–27.

Walker, I., et al (2013). Energy implications of in-line filtration in California homes. *ASHRAE Transactions*, *119*(PART 2), 399–417.

Wang, C. Sen, et al (2013). Removal of nanoparticles from gas streams by fibrous filters: A review. *Industrial and Engineering Chemistry Research*, *52*(1), 5–17.

Wu, T., et al (2020). Characterization of a thermal aerosol generator for HVAC filtration experiments (RP-1734). *Science and Technology for the Built Environment*, *26*(6), 816–834.

Wu, T., et al (2021). Urban aerosol size distributions: A global perspective. *Atmospheric Chemistry and Physics*, *21*(11), 8883–8914.

Zaatari, M., et al (2014). The relationship between filter pressure drop, indoor air quality, and energy consumption in rooftop HVAC units. *Building and Environment*, *73*, 151–161.

Zhang, Y., et al (2020). Investigating the impact of filters on long-term particle concentration measurements in residences (RP-1649). *Science and Technology for the Built Environment*, *26*(8), 1037–1047.

ACKNOWLEDGEMENTS

Financial support was provided by the American Society of Heating, Refrigerating, and Air-Conditioning Engineers (ASHRAE RP-1734). The authors are grateful for the support of the Project Monitoring Subcommittee: Paolo Tronville, Geoff Crosby, Bruce McDonald, Tom Justice, and Brian Krafthefer. The authors thank Dr. Ayesha Shah and David Rater for their assistance with overseeing the HVAC filter test rig and associated safety protocol for its operation.